Tests for contamination of the HRMA

Molecular contamination

AXAF Project Science

AXAF XRCF Pre-Calibration Review

NASA Marshall Space Flight Center

1996 November 13-15

Summary

Molecular contamination can alter HRMA performance.

- Reflectance of hydrocarbon differs from that of iridium.
  - Change in effective area is as high as 0.5% (I_{hc}/Å).
  - At most energies, hydrocarbon contamination increases effective area.
  - Change in effective area is most pronounced at Ir-M_V edge.
- Droplet-like molecular contamination scatters like particulates

Primary test for molecular contamination is an SSD measurement of the HRMA effective area of each HRMA shell.

Secondary tests are parasitic or conditional.

- HETG spectra could probe properties of contamination.
  - Spectra would show details of Ir-M_V edge.
  - Spectra might show atomic edges of contaminants.
- SSD measurements of HRMA-subaperture effective areas could identify azimuthal location of detected molecular contamination.

Primary test

Operating XSS source is the Electron Impact Point Source (EIPS).

- Carbon (C) anode is at 15 kV, with 1.5% bias and 0.4 mA current.
- Filter wheel position is for the beryllium τ=2 [BeK2] filter.

Relevant monitor detector is the Building-500 Solid-State Detector SSD_5.

- Shaping time constant is set to 2 µs for up to 10,000 ct/s.
- Selected aperture diameter is the 5 mm (no Al filter).

Focal-plane detector is the Solid-State Detector SSD_X.

- Shaping time constant is set to 2 µs for up to 10,000 ct/s.
- Selected aperture diameter is the 5 mm (no Al filter).

Configure HRMA for spectrometric effective-area measurement.

- Stow OTGs.
- Sequentially set HRMA shutters to obtain 300-s SSD spectra for each HRMA shell.

Effective area of HRMA with hydrocarbon layer

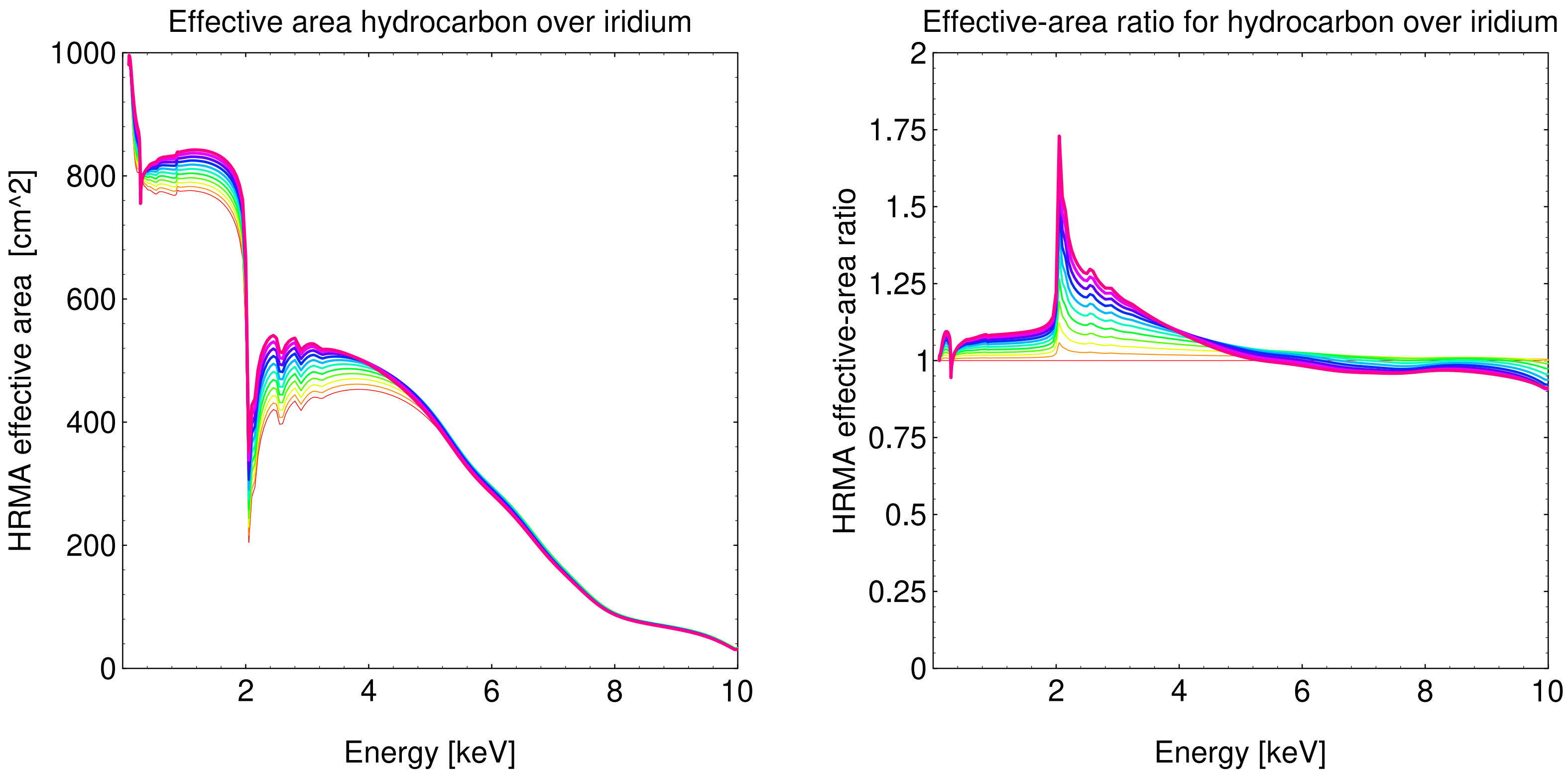

Effective area (A_{eff}) of the HRMA for various thicknesses of a hydrocarbon film. The plots show (l) the effective area and (r) the effective-area ratio for hydrocarbon thickness (l_{hc}) ranging from 0 Å to 50 Å, in 5-Angstrom increments.

Effective area of HRMA shell 1 with hydrocarbon layer

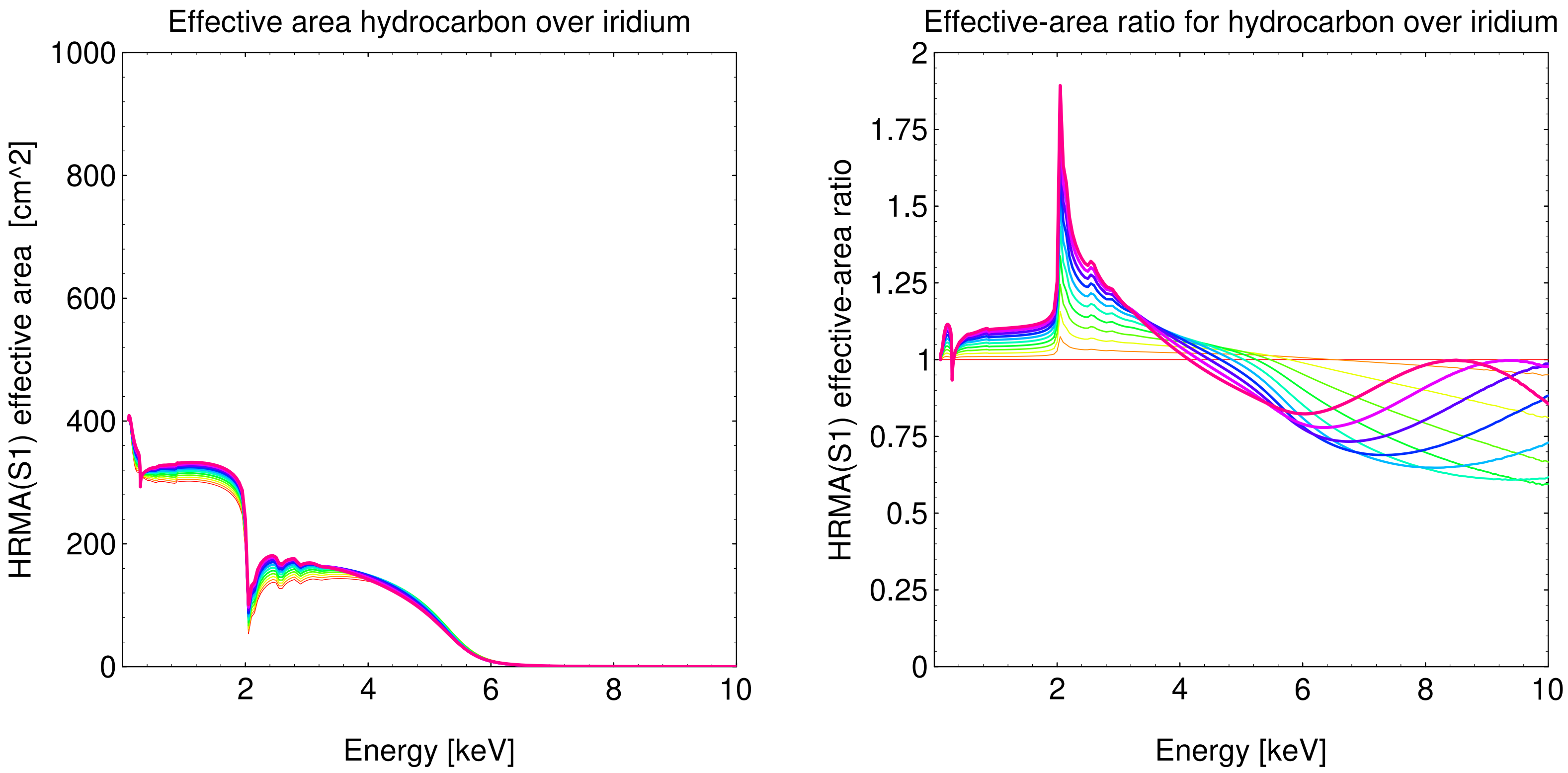

Effective area (A_{eff}) of the HRMA shell 1 for various thicknesses of a hydrocarbon film. The plots show (l) the effective area and (r) the effective-area ratio for hydrocarbon thickness (l_{hc}) ranging from 0 Å to 50 Å, in 5-Angstrom increments.

Effective area of HRMA shell 3 with hydrocarbon layer

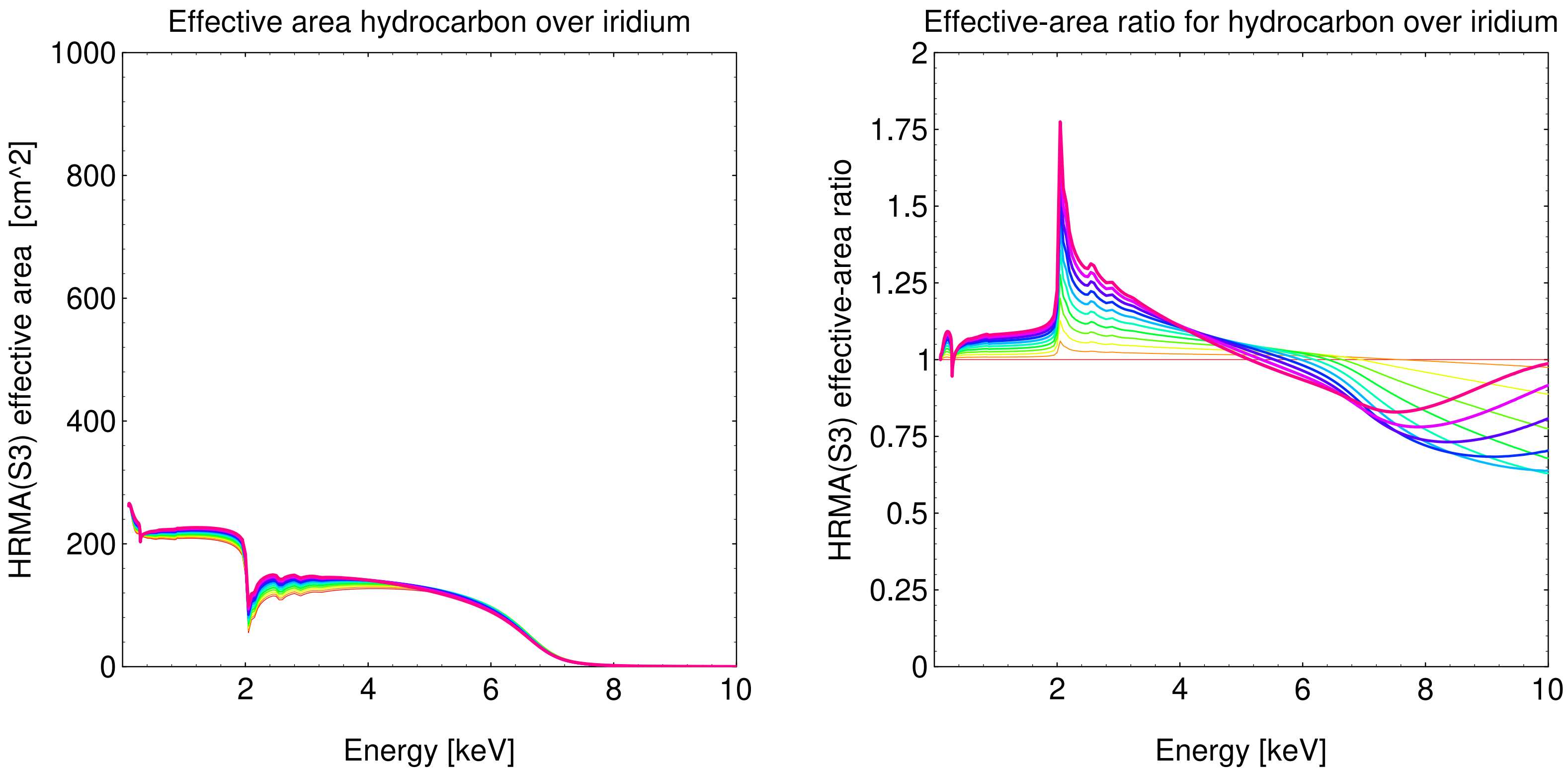

Effective area (A_{eff}) of the HRMA shell 3 for various thicknesses of a hydrocarbon film. The plots show (l) the effective area and (r) the effective-area ratio for hydrocarbon thickness (l_{hc}) ranging from 0 Å to 50 Å, in 5-Angstrom increments.

Effective area of HRMA shell 4 with hydrocarbon layer

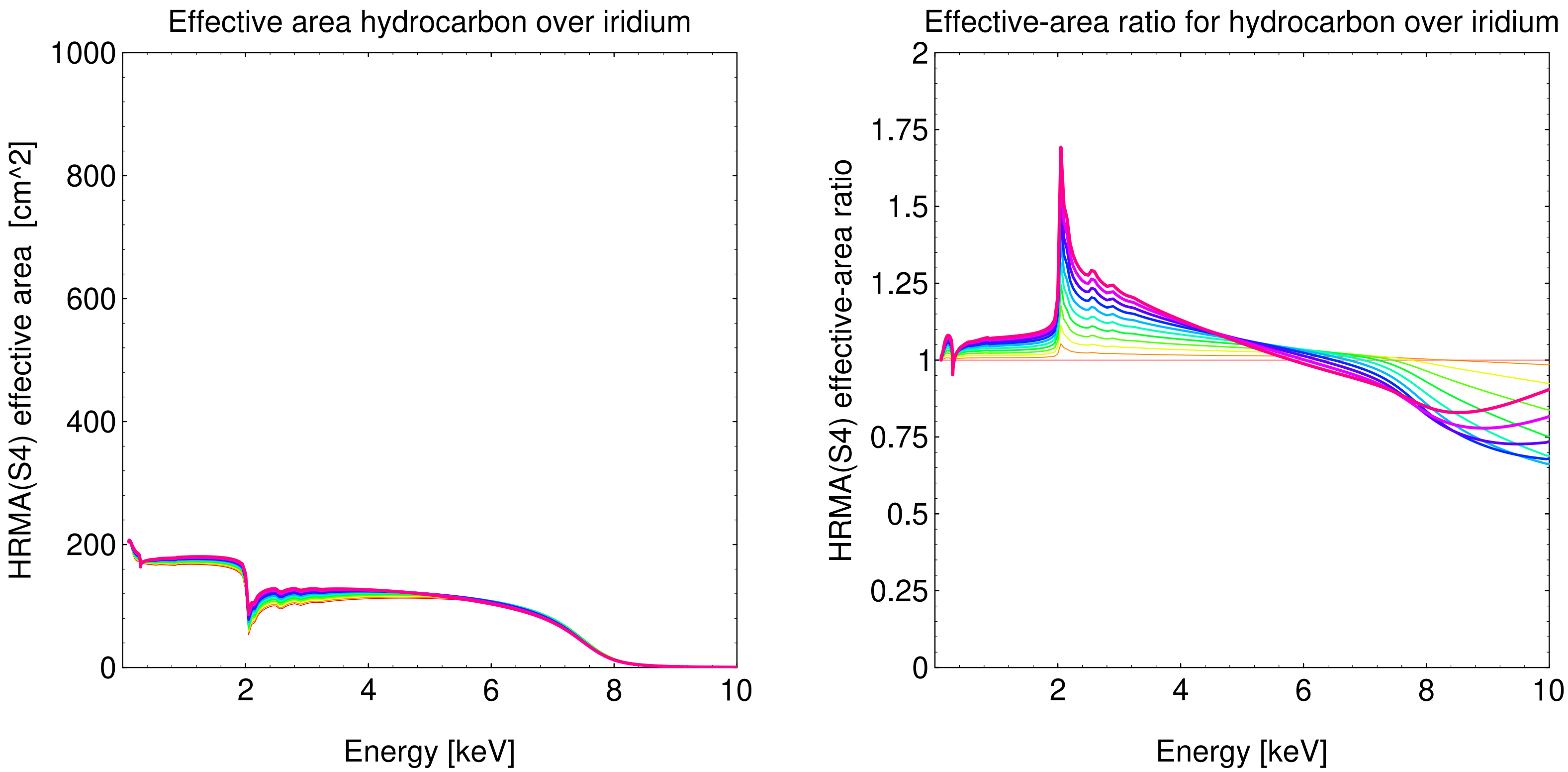

Effective area (A_{eff}) of the HRMA shell 4 for various thicknesses of a hydrocarbon film. The plots show (l) the effective area and (r) the effective-area ratio for hydrocarbon thickness (l_{hc}) ranging from 0 Å to 50 Å, in 5-Angstrom increments.

Effective area of HRMA shell 6 with hydrocarbon layer

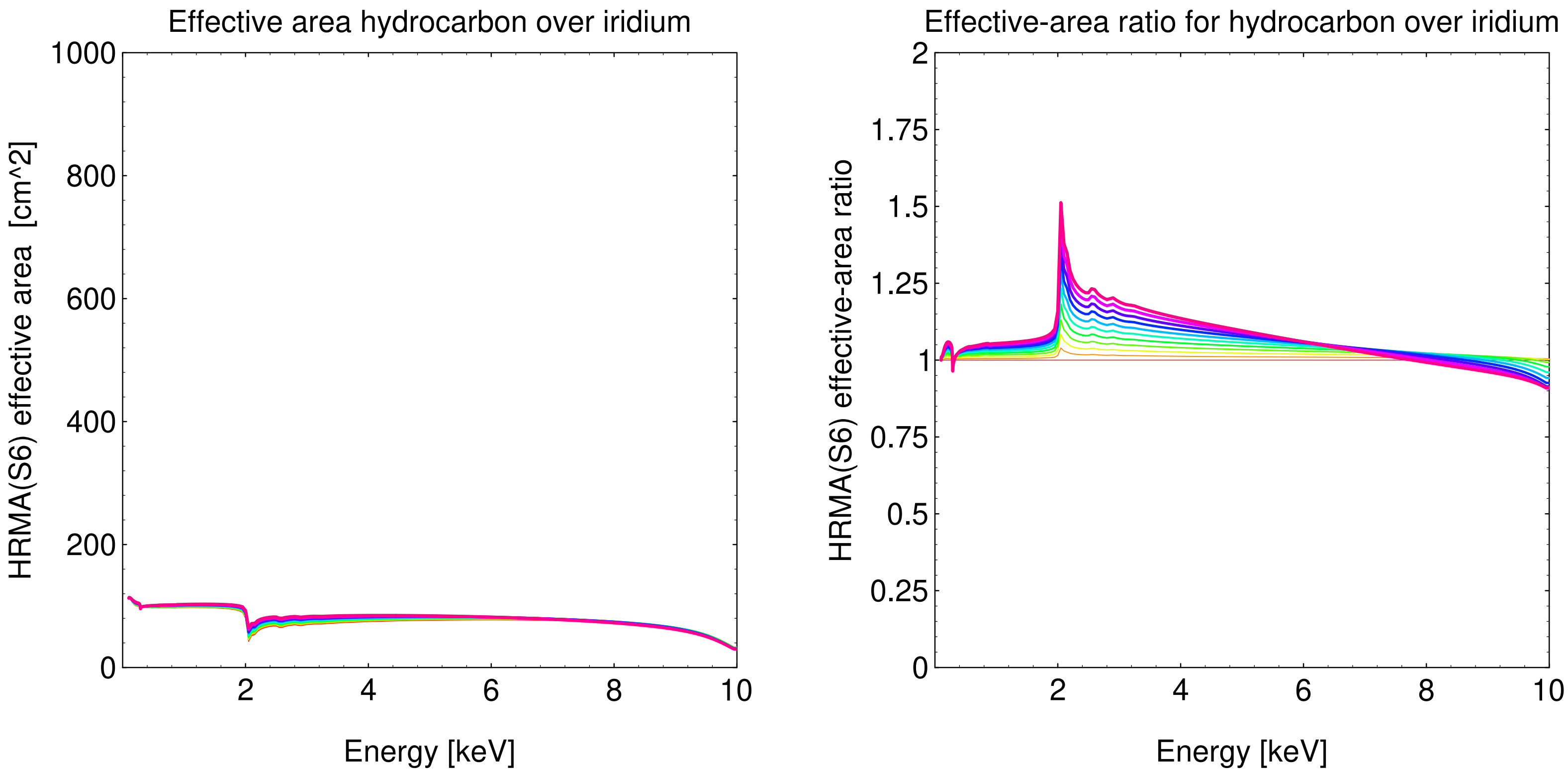

Effective area (A_{eff}) of the HRMA shell 6 for various thicknesses of a hydrocarbon film. The plots show (l) the effective area and (r) the effective-area ratio for hydrocarbon thickness (l_{hc}) ranging from 0 Å to 50 Å, in 5-Angstrom increments.

Contamination sensitivity measurement for HRMA shell 1

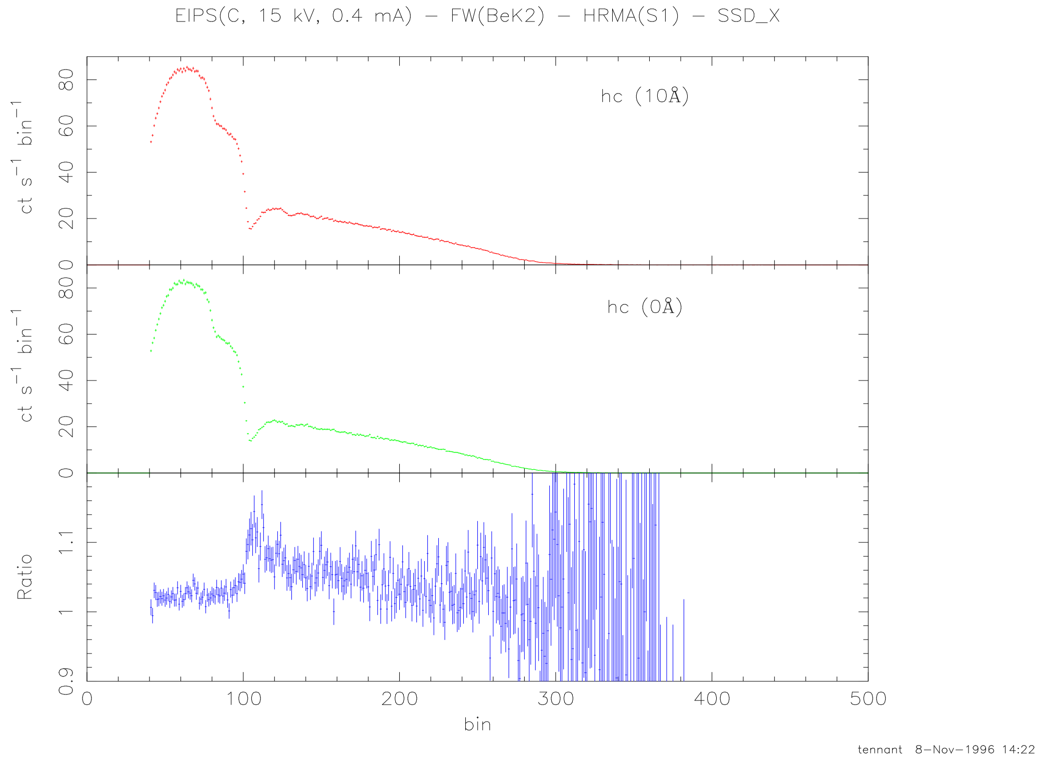

Simulated 300-s contamination sensitivity measurement for HRMA shell 1. The plots show the SSD_X pulse-height spectrum for 0-Å hydrocarbon layer, the spectrum for 10-Å hydrocarbon layer, and the ratio. Each bin is 4 SSD channels or 19.5 eV.

Contamination sensitivity measurement for HRMA shell 3

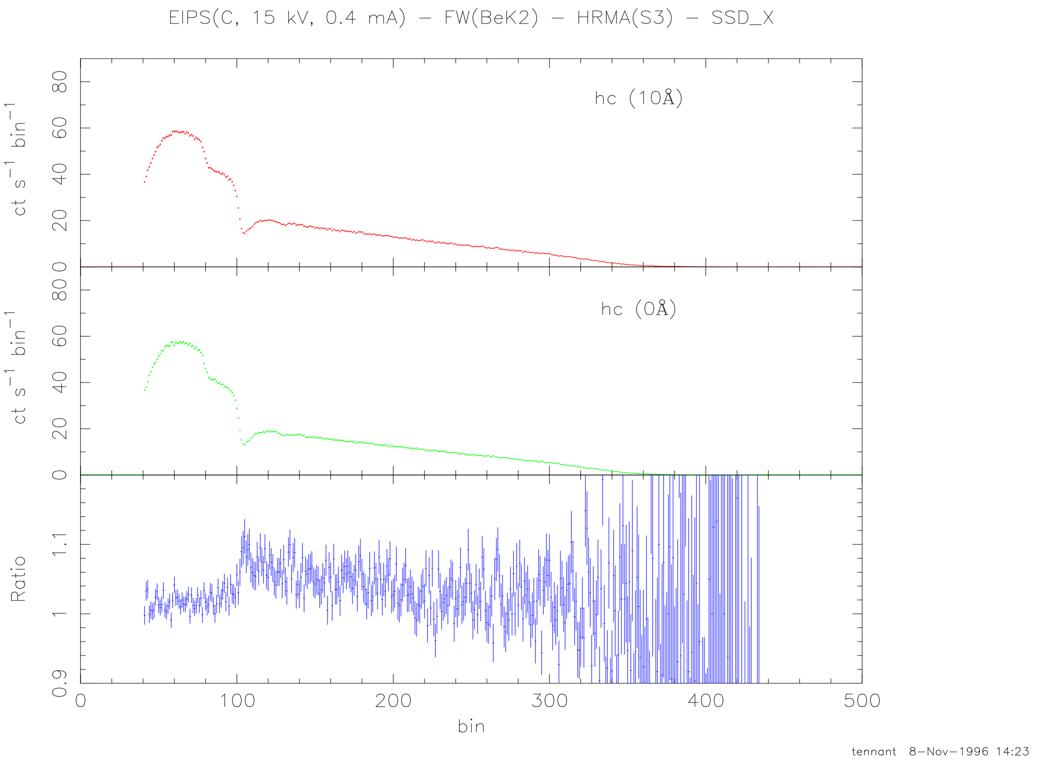

Simulated 300-s contamination sensitivity measurement for HRMA shell 3. The plots show the SSD_X pulse-height spectrum for 0-Å hydrocarbon layer, the spectrum for 10-Å hydrocarbon layer, and the ratio. Each bin is 4 SSD channels or 19.5 eV.

Contamination sensitivity measurement for HRMA shell 4

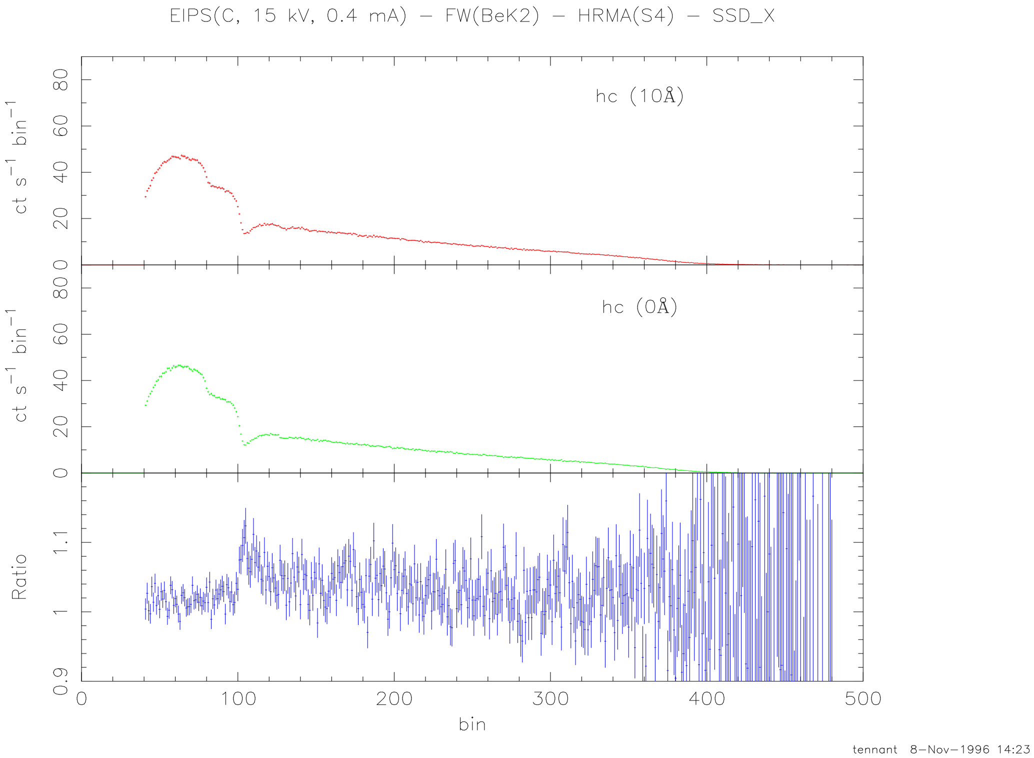

Simulated 300-s contamination sensitivity measurement for HRMA shell 4. The plots show the SSD_X pulse-height spectrum for 0-Å hydrocarbon layer, the spectrum for 10-Å hydrocarbon layer, and the ratio. Each bin is 4 SSD channels or 19.5 eV.

Contamination sensitivity measurement for HRMA shell 6

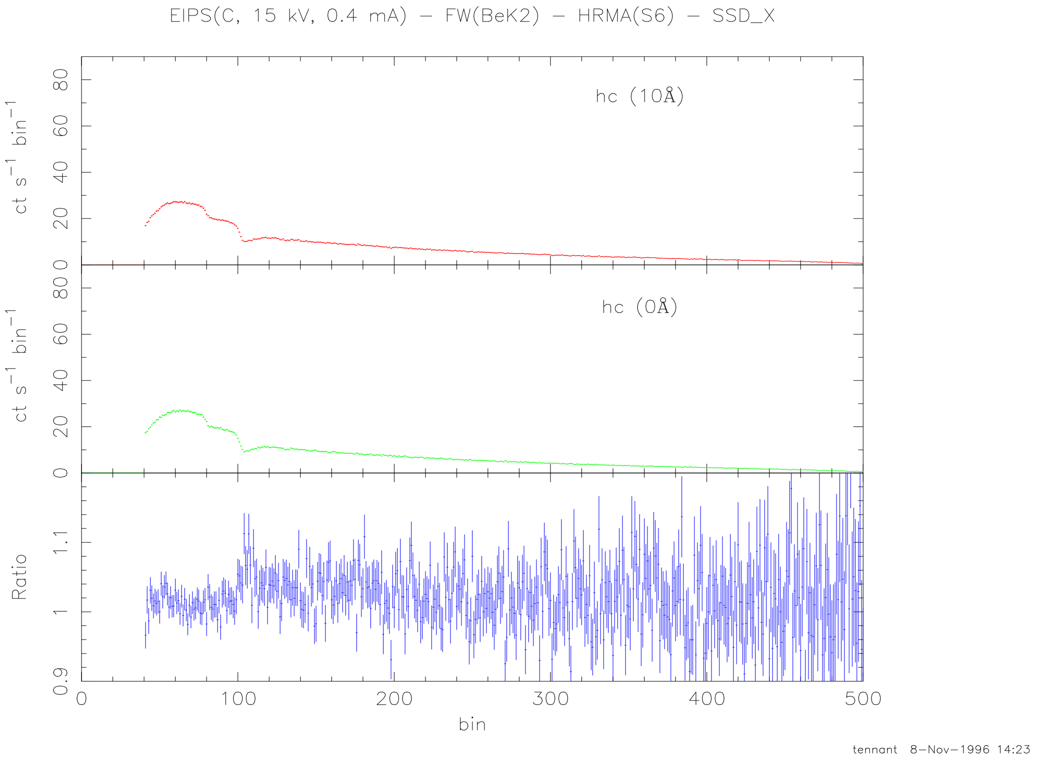

Simulated 300-s contamination sensitivity measurement for HRMA shell 6. The plots show the SSD_X pulse-height spectrum for 0-Å hydrocarbon layer, the spectrum for 10-Å hydrocarbon layer, and the ratio. Each bin is 4 SSD channels or 19.5 eV.

Effective area measurement for HRMA shell 1

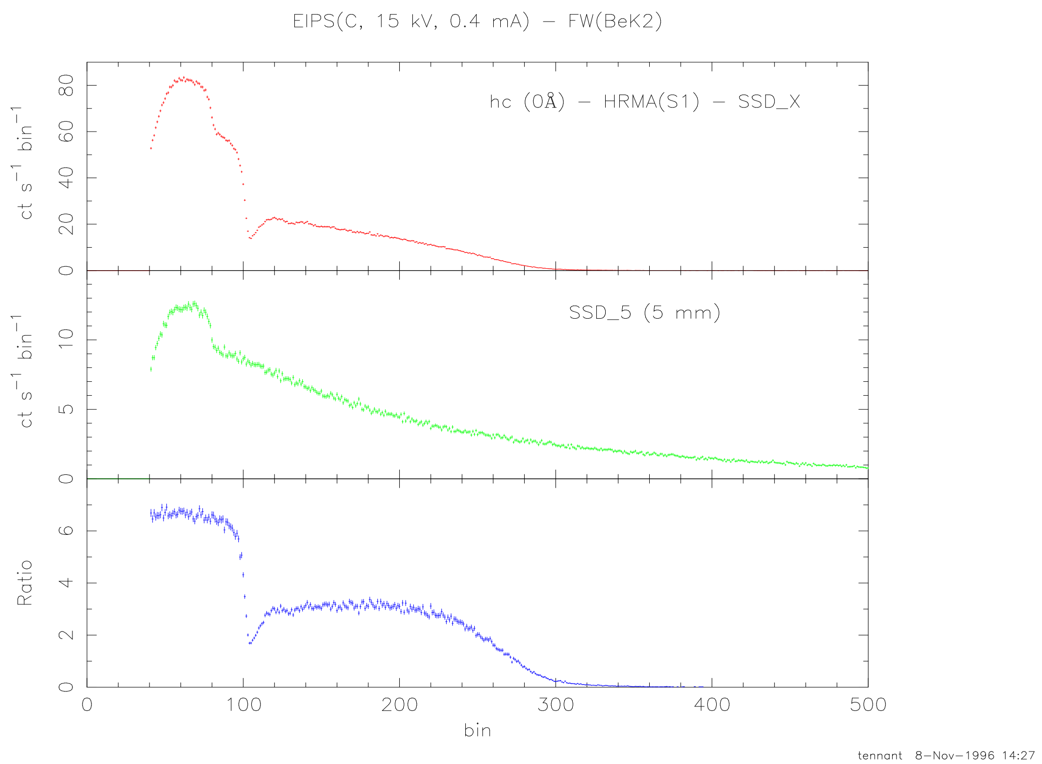

Simulated 300-s effective-area (A_{eff}) measurement for HRMA shell 1. The plots show the SSD_X pulse-height spectrum, the SSD_5 pulse-height spectrum, and the ratio. Each bin is 4 SSD channels or 19.5 eV. The shell-1 A_{eff} is 44.2 cm^2 times the ratio.

Effective area measurement for HRMA shell 3

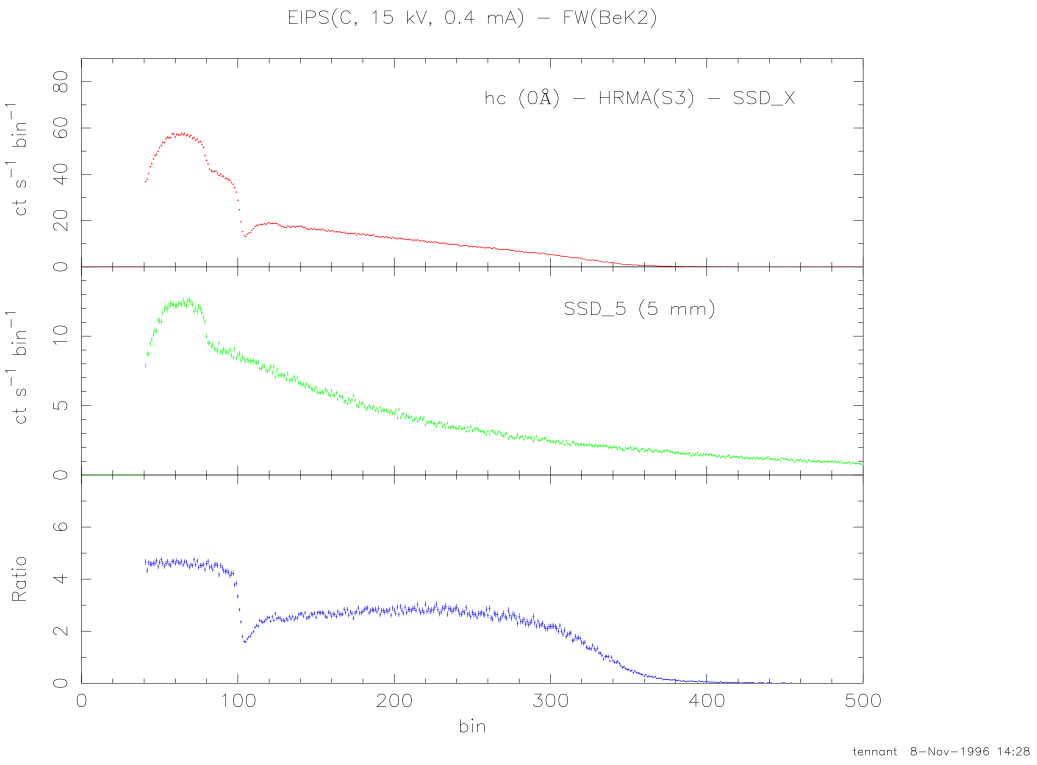

Simulated 300-s effective-area (A_{eff}) measurement for HRMA shell 3. The plots show the SSD_X pulse-height spectrum, the SSD_5 pulse-height spectrum, and the ratio. Each bin is 4 SSD channels or 19.5 eV. The shell-3 A_{eff} is 44.2 cm^2 times the ratio.

Effective area measurement for HRMA shell 4

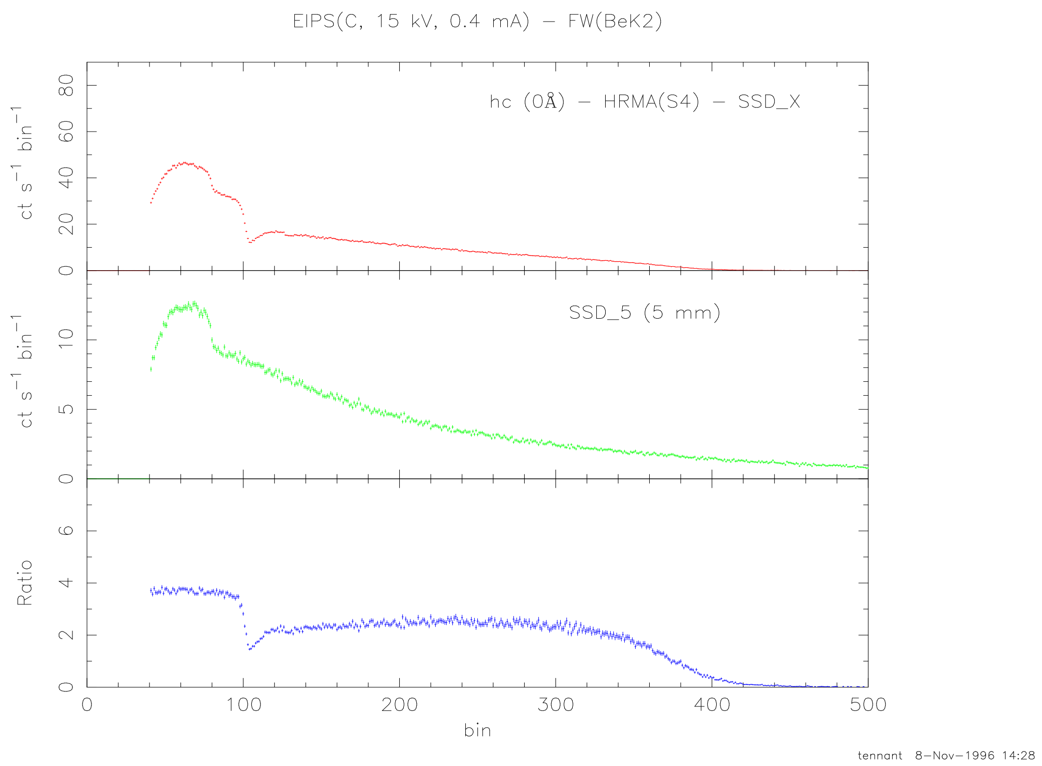

Simulated 300-s effective-area (A_{eff}) measurement for HRMA shell 4. The plots show the SSD_X pulse-height spectrum, the SSD_5 pulse-height spectrum, and the ratio. Each bin is 4 SSD channels or 19.5 eV. The shell-4 A_{eff} is 44.2 cm^2 times the ratio.

Effective area measurement for HRMA shell 6

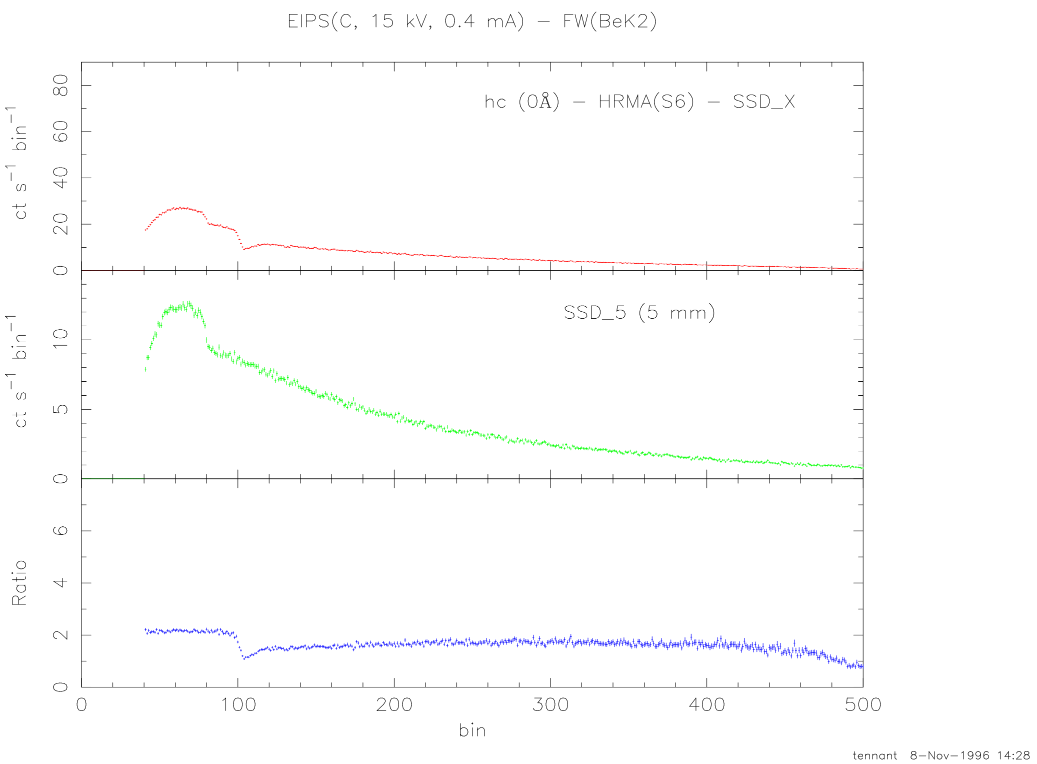

Simulated 300-s effective-area (A_{eff}) measurement for HRMA shell 6. The plots show the SSD_X pulse-height spectrum, the SSD_5 pulse-height spectrum, and the ratio. Each bin is 4 SSD channels or 19.5 eV. The shell-6 A_{eff} is 44.2 cm^2 times the ratio.